

## Measurements of Cosmic-Ray Lithium and Beryllium Isotopes with the PAMELA-Experiment

W. MENN<sup>1</sup> FOR THE PAMELA COLLABORATION

<sup>1</sup>Universität Siegen, FB Physik, Walter-Flex-Str. 3, 57068 Siegen

menn@pamela.physik.uni-siegen.de

**Abstract:** On the 15th of June 2006, the PAMELA satellite-borne experiment was launched from the Baikonur cosmodrome and it has been collecting data since July 2006. The apparatus comprises a time-of-flight system, a silicon-microstrip magnetic spectrometer, a silicon-tungsten electromagnetic calorimeter, an anticoincidence system, a shower tail counter scintillator and a neutron detector. The scientific objectives addressed by the mission are the measurement of the antiprotons and positrons spectra in cosmic rays, the hunt for antinuclei as well as the determination of light nuclei fluxes from hydrogen to oxygen in a wide energy range and with very high statistics. In this paper the identification capability for light nuclei isotopes (especially lithium and beryllium) using multiple  $dE/dx$  measurements in the calorimeter and first results of the isotopic ratio will be presented.

**Keywords:** cosmic rays

### 1 Introduction

Measurements of the isotopic composition of elements of the cosmic radiation provide significant constraints on cosmic ray source composition and cosmic ray transport and acceleration in the galaxy. The isotopes of Li, Be, and B in cosmic rays are pure spallation products of primary cosmic rays, mainly C, N, and O, when they interact with interstellar matter during their propagation in the Galaxy. For example, the production of <sup>7</sup>Li in particular has important cosmological implications. The abundance of the radioactive secondary isotope <sup>10</sup>Be (half-life:  $1.5 \times 10^6$  years) is another very important measurement to be made in this field. Object of this paper is the description of the work in progress on the identification capability of the PAMELA instrument for light nuclei isotopes (especially lithium and beryllium) using multiple  $dE/dx$  measurements in the calorimeter.

### 2 The PAMELA instrument

The PAMELA experiment is performed by an international collaboration of scientists from Italy, Russia, Germany and Sweden.

The PAMELA apparatus, shown in figure 1, is composed of several sub-detectors: TOF system, anticoincidence system (CARD, CAS, CAT), magnetic spectrometer with microstrip silicon tracking system, W/Si electromagnetic imaging calorimeter, shower-tail-catcher scintillator (S4) and neutron detector.

A detailed description of the PAMELA instrument and an

overview of the mission can be found in [1]. The instrument has a maximum diameter of 102 cm and height of 120 cm; its mass is 470 kg, the maximum power consumption is 355 W. The core of the instrument is a magnetic spectrometer, made of a permanent magnet (0.43 T) and a silicon tracking system (resolution in the bending side  $4 \mu\text{m}$ ) for a maximum detectable rigidity of 1 TV. The dimensions of the permanent magnet define the geometrical factor of the PAMELA experiment to be  $21.5 \text{ cm}^2\text{sr}$ . The magnetic spectrometer determines the charge sign and momentum of the incoming particle through the trajectory reconstruction in the magnetic field. Due to the small dimensions of the track detector, the silicon planes need no further support structure, which minimizes the effect of multiple scattering at low energies. Thus the momentum resolution for lithium and beryllium nuclei is better than 4% between 2 GV and 20 GV. A time-of-flight system consisting of three double layers (S1, S2, S3) of segmented plastic scintillator provides timing and  $dE/dx$  measurements and defines the primary PAMELA trigger; it will also identify downward-going particles.

The W/Si sampling imaging calorimeter comprises 44 single-sided silicon strip detector planes interleaved with 22 plates of tungsten absorber [2]. Each tungsten layer has a thickness of 0.74 radiation lengths (2.6 mm) and it is sandwiched between two printed circuit boards, which house the silicon detectors as well as the frontend and digitizing electronics. Each silicon plane consists of  $3 \times 3$ ,  $380 \mu\text{m}$  thick,  $8 \times 8 \text{ cm}^2$  detectors, segmented into 32 strips with a pitch of 2.4 mm. The orientation of the strips for two consecutive silicon planes is shifted by 90, thus providing 2-dimensional spatial information. Each of the 32 strips

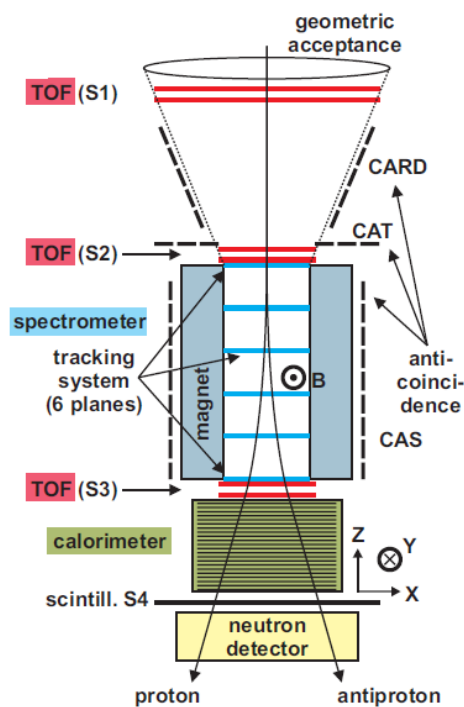


Figure 1: The PAMELA instrument

is wire-bonded to the corresponding strip on the other two detectors in the same row (or column), thereby forming 24 cm long readout strips. The total depth of the calorimeter is 16.3 radiation lengths and 0.6 nuclear interaction lengths. The high granularity of the calorimeter and the use of silicon strip detectors provide detailed information on the longitudinal and lateral profiles of particles interactions as well as a measure of the deposited energy.

The main purpose of the instrument is the separation between hadronic and leptonic components, which is provided by the velocity measurement (obtained from the trajectory and time-of-flight) at lower energies and by an imaging W/Si detector and a neutron counter for kinetic energies above 1 GeV. More technical details can be found in [1]. PAMELA has been inserted in a pressurized vessel and installed on board the Russian satellite DK-1 dedicated to Earth observation. It was launched on June 15th 2006 by a Soyuz-U rocket from the Baikonur cosmodrome in Kazakhstan in an elliptical orbit, ranging between 350 and 610 km and with an inclination of 70 degrees. Since July 2006 PAMELA is delivering daily 16 Gigabytes of data to the Ground Segment in Moscow.

### 3 Data Analysis

#### 3.1 Particle Selection

A particle traversing the PAMELA apparatus crosses, in the standard trigger configuration, six layers of plastic scintillators, six silicon tracker layers and, at least, the first silicon

plane of the calorimeter. In this way the three different sub-detectors are able to identify light nuclei with different efficiencies, resolutions and Z ranges. To select non interacting nuclei above the calorimeter, we applied the following selection cuts:

- single reconstructed track in the spectrometer with a good  $\chi^2$  for the fitted track.
- A geometrical cut to ensure that particle is inside the acceptance of the apparatus
- Less than three paddles hit on each of the six scintillator layers.
- Consistent charge selection with TOF layers

These selection criteria are still under development and are also used for the analysis of the secondary to primary charge ratios [3] which will be also presented in this conference. The isotopic analysis of nuclei with the calorimeter is restricted to events which do not interact inside the calorimeter. These events are selected by applying selection cuts on the ratio between the energy deposited in the strip closest to the track and the neighboring strip on each side and the total energy detected, for non interacting events this ratio is of course equal to one.

The probability to survive the passage through the calorimeter depends on the particles charge and mass, thus the isotopic ratio derived from the data needs to be corrected. We have developed a GEANT 4 simulation of the full calorimeter for this task and for a detailed comparison of simulated data and flight data.

#### 3.2 Isotope Identification

As described above, the calorimeter comprises 44 single-sided silicon strip detector planes interleaved with 22 plates of tungsten absorbers. Using the energy loss in the silicon, one aims to get a precise measurement of the energy loss of the particle. In a single silicon layer, the energy loss distributions shows a Landau tail which degrades the resolution of the  $dE/dx$  measurement. Using a truncation method, the 50% of samples with larger pulse amplitudes are excluded before taking the mean of the  $dE/dx$  measurements, thus reducing the effect of the Landau tail. The principle is shown in figure 2 for a typical  $Z=3$  event. The circles show the energy loss (in MIP) in each of the silicon layers, the filled circles survive if 50% of the highest measurements are removed. These remaining measurements are used to calculate a mean energy loss value.

In figure 3 we select  $Z=2$  particles and plot the mean  $dE/dx$  for each event vs. the rigidity measured with the magnetic spectrometer. The energy loss in MeV was derived from the measurement in MIP using a conversion factor. One can see that a good isotope separation can be reached up to about 4 GV for helium. As an example we show the helium data in a rigidity interval between 2.5 and 2.7 GV in figure 4. The isotope resolution (about 5%) is better than

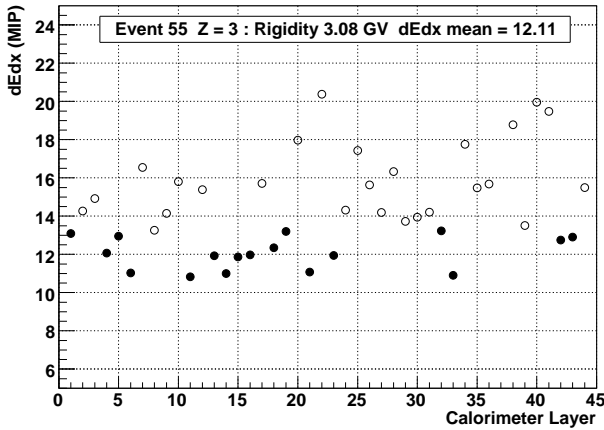


Figure 2: Energy loss in the calorimeter layers for a typical  $Z=3$  event

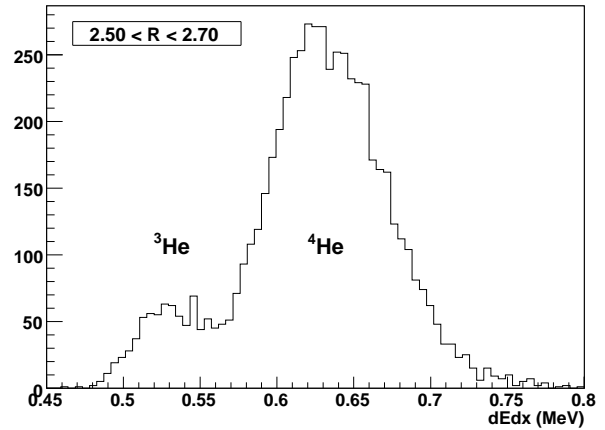


Figure 4: Helium isotope resolution between 2.5 and 2.7 GV

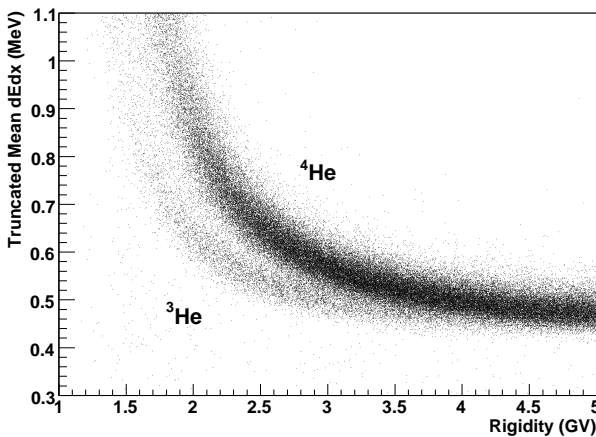


Figure 3: Helium isotope resolution

using the velocity information from the TOF and the rigidity from the magnetic spectrometer, an analysis which is also in progress and which will be presented at this conference. We will use hydrogen and helium data to cross-check the two procedures.

In figure 2 the energy loss in the silicon layers was shown. In this example the particle went through the calorimeter without major slowdown, the single energy loss measurements do not show a big increase. For lower rigidities the slowdown of the particle becomes important, the energy loss increases when going deeper in the calorimeter. If one just cuts on 50% of the highest signals, this will preferentially remove the measurements from the lower layers. Our recent analysis shows that one still gets good results taking the mean of the remaining (mostly upper) layers. A modified approach of the method is to divide the full calorimeter in several subsections, for example 4 parts with 11 layers. In each of the 4 parts one cuts away the highest signals and

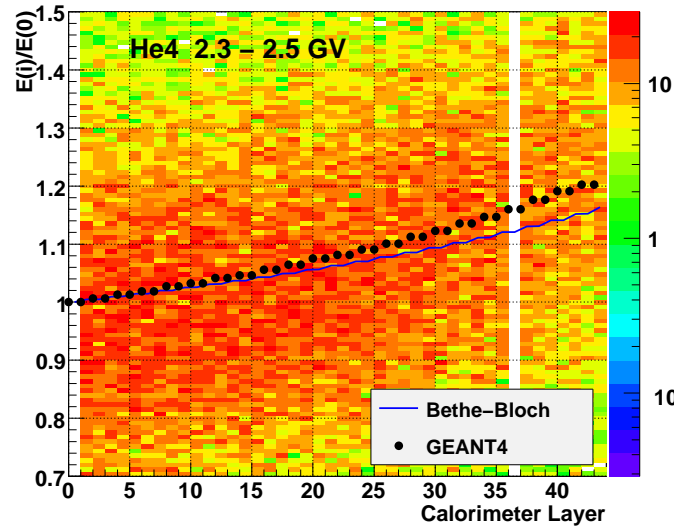


Figure 5: The value of  $E(i)/E(0)$  for  $^4\text{He}$  pre-selected with the TOF

afterwards takes the mean of the remaining layers. In this way also the lower part of the calorimeter is used. One can also think of trying to fit the slowdown of the particle with some model, using this additional information to improve further the isotope resolution. As an example, in figure 5 we show the ratio  $E(i)/E(0)$  ( $E(i)$  is the energy loss in the  $i$ -th layer,  $E(0)$  is the energy loss in the first layer) for each layer for  $^4\text{He}$  in the rigidity interval between 2.3 - 2.5 GV. We used the TOF to pre-select  $^4\text{He}$  from the flight data. The rise in the energy loss due to the slowdown of the particle is clearly to see. The blue line represents an analytical calculation using the Bethe-Bloch equation. The black circles are the result of the GEANT4 simulation, which seems to describe very well the data.

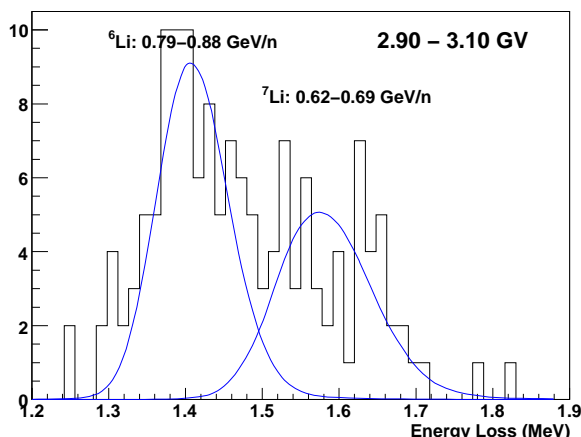


Figure 6: Lithium isotope resolution between 2.9 and 3.1 GV

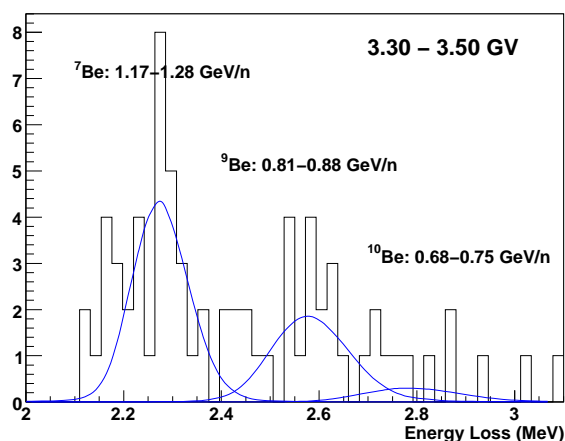


Figure 7: Beryllium isotope resolution between 3.3 and 3.5 GV

Using the high statistics of hydrogen and helium flight data, we will be able to tune the parameters of the simulation to match the data. For lithium and beryllium data, where the statistics is much lower, we will then use the simulation to derive the isotopic ratio.

As an example, we show the distribution of the mean  $dE/dx$  for lithium in the rigidity interval between 2.9 and 3.1 GV in figure 6. The blue line shows a preliminary fit using the GEANT 4 simulation at the present stage. In figure 7 we show the distribution of the mean  $dE/dx$  for beryllium in the rigidity interval between 3.3 and 3.5 GV. Also in this figure the blue line shows a preliminary fit using the GEANT 4 simulation. Though the statistics is low,  ${}^7\text{Be}$  and  ${}^9\text{Be}$  are easily separated. The separation of  ${}^9\text{Be}$  and  ${}^{10}\text{Be}$  seems challenging, but the analysis is ongoing.

Isotopic abundance will then be estimated by examining the  $dE/dx$  distributions at fixed rigidity described by distri-

bution derived from the simulation. In order to have isotopic ratios as functions of kinetic energy, instead of rigidity, we will fix the kinetic energy bins of the final ratio and calculate the corresponding rigidity intervals for each species. Two different rigidity binning (one for each isotope) are selected in such a way that the  $n$ -th rigidity bin will always correspond to the same kinetic energy range. In doing isotopic ratios as functions of rigidity all selection efficiencies simplify and do not contribute to the ratio value, however this is not true when working in kinetic energy since, as stated before, the same kinetic energy range corresponds to different rigidity ranges according to which particle are we considering. A correction for the different efficiencies will be applied in evaluating the ratios. The cut efficiencies (single track, fiducial volume traversed, minimum number of hits on the bending view, minimum lever arm,  $\chi^2$ ) have been carefully estimated using both experimental and simulated data. Extensive Monte Carlo simulations (GEANT4+QGSP BIC) have been carried out in order to estimate with low statistical errors track efficiencies, correction to geometrical factors and contaminations [4].

## 4 Conclusion

We have presented the work in progress on the identification capability of the PAMELA instrument for light nuclei isotopes (especially lithium and beryllium) using multiple  $dE/dx$  measurements in the calorimeter. The results on hydrogen and helium are promising, giving a mass resolution in the order of 5 % around 1 GeV/nuc. We expect to provide new data of the  ${}^6\text{Li}$  and  ${}^7\text{Li}$  isotopes as well as for the  ${}^7\text{Be}$  and  ${}^9\text{Be}$  isotopes up to about 1.5 GeV/n. Also the separation of  ${}^9\text{Be}$  and  ${}^{10}\text{Be}$  seems possible. The different approaches to analyze the data need to be compared, also the GEANT 4 simulation needs to be optimized. We will present updated results at the conference.

## 5 Acknowledgments

The GEANT4 simulation is carried out by Ioffe Institute (St.Petersburg) with support of the Russian Foundation for Basic Research Grant 10-02-00347

## References

- [1] Picozza P. et al., *Astropart. Phys.*, 2007, **27**, 296-315.
- [2] Boezio M. et al., *Nucl. Instr. and Meth. A*, 2002, **487** 407-422
- [3] Osteria G. et al., *Proc. 31st Int. Cosmic Ray Conf. (Lodz)*, 2009
- [4] De Santis C. et al., PAMELA measurements of boron and carbon spectra in the energy range 100MeV/n - 100GeV/n, this conference